JMB

Available online at www.sciencedirect.com

SCIENCE $\overset{d}{\mathbf{\mathscr{d}}}$ DIRECT®

ELSEVIER

Latent LytM at 1.3 Å Resolution

Sergey G. Odintsov[1,2]†, Izabela Sabala[1,2]†, Malgorzata Marcyjaniak[1,2] and Matthias Bochtler[1,2]*

[1]*International Institute of Molecular and Cell Biology, ul. Trojdena 4, 02-109 Warsaw Poland*

[2]*Max-Planck-Institute for Molecular Cell Biology and Genetics, Pfotenhauerstr. 108 01309 Dresden, Germany*

LytM, an autolysin from *Staphylococcus aureus*, is a Zn^{2+}-dependent glycyl-glycine endopeptidase with a characteristic HxH motif that belongs to the lysostaphin-type (MEROPS M23/37) of metallopeptidases. Here, we present the 1.3 Å crystal structure of LytM, the first structure of a lysostaphin-type peptidase. In the LytM structure, the Zn^{2+} is tetrahedrally coordinated by the side-chains of N117, H210, D214 and H293, the second histidine of the HxH motif. Although close to the active-site, H291, the first histidine of the HxH motif, is not directly involved in Zn^{2+}-coordination, and there is no water molecule in the coordination sphere of the Zn^{2+}, suggesting that the crystal structure shows a latent form of the enzyme. Although LytM has not previously been considered as a proenzyme, we show that a truncated version of LytM that lacks the N-terminal part with the poorly conserved Zn^{2+} ligand N117 has much higher specific activity than full-length enzyme. This observation is consistent with the known removal of profragments in other lysostaphin-type proteins and with a prior observation of an active LytM degradation fragment in *S. aureus* supernatant. The "asparagine switch" in LytM is analogous to the "cysteine switch" in pro-matrix metalloproteases.

Corresponding author

Introduction

Metallopeptidases can often be recognised by the presence of a short conserved signature sequence containing histidine and glutamate residues. The most common motif is HExxH ("zinzins"), but other motifs such as HxxEH ("inverzincins"), HxxE ("carboxypeptidase family") and HxH (e.g. lysostaphin-like) have also been described.[1]

HxH metalloproteases of the lysostaphin-type of peptidases occur in bacteriophages, in Gram-positive and in Gram-negative bacteria. One member sequence has also been found in *Anopheles gambiae*, the African malaria mosquito.[2] The proteases from bacteriophages and Gram-positive bacteria have been studied most, and were shown to have a preference for peptides containing polyglycine residues, especially Gly-Gly-Xaa, where Xaa is any aliphatic hydrophobic residue.[3] This specificity is consistent with their physiological role: lysosta-

phin-like peptidases from bacteriophages and Gram-positive bacteria cleave polyglycine cross-bridges in the peptidoglycan of Gram-positive bacterial cells.[3] Their role in Gram-negative bacteria is less clear: some peptidases, like β-lytic protease from *Achromobacter lyticus*, target cell walls of Gram-positive bacteria, possibly providing a competitive advantage to the producer organism.[4] Others seem to have additional roles, like LasA from *Pseudomonas aeruginosa* that is believed to participate in host elastin degradation.[5]

Lysostaphin-type peptidases from Gram-positive bacteria appear to share the affinity for glycine-rich peptides. Nevertheless, some of them show remarkable specificity. For example, it is known that *Staphylococcus simulans* cell walls are resistant to lysostaphin, which they produce, and that this resistance is mediated by an increase in the serine and a decrease in the glycine content of the bacterial cell wall.[6] In many cases, the presence of lysostaphin-type proteins is coupled with the presence of a self-resistance mechanism. A good example is the millericin B operon from *Streptococcus milleri*: the operon encodes millericin B, a peptidoglycan hydrolase, and several other proteins that add a leucine to the polyglycine

---

precursor and thus contribute to self-protection of the producer strain.[7]

Although such arrangements are common, there are also many cases of lysostaphin-like peptidoglycan hydrolases that can degrade the cell walls of the producer organism at least *in vitro*. Such peptidoglycan hydrolases are known as autolysins.[8] Although functional redundancy in autolysins has made it difficult to assign specific functions to individual enzymes, autolysins are believed to be involved in vegetative growth, peptidoglycan maturation, cell wall expansion, cell wall turnover and protein secretion.[8]

LytM is an autolysin that was originally identified in an autolysis defective mutant of *Staphylococcus aureus*.[9] Based on its similarity to lysostaphin, the enzyme would be expected to be specific for glycine-rich sequences, a conclusion that is supported by the experimental data. Ramadurai *et al*.[10] report that the enzyme releases free amino groups, but not reducing sugars from staphylococcal cell walls, supporting its classification as a protease. Moreover, it degrades the cell walls from *S. carnosus*, but not those from *Micrococcus luteus*, leading the authors to speculate that the enzyme is a glycyl-glycine endopeptidase. LytM activity can easily be assayed by zymography with purified cell walls as the substrate. Intriguingly, LytM preparations from both native and recombinant sources have been reported to give rise to three bands in zymography, one band corresponding to the full-length enzyme, and two bands of lower molecular mass that were considered as degradation products.[9]

LytM and other lysostaphin-type proteins do not share significant sequence similarity with other peptidase families of known structure. In spite of the widespread *in vitro* use of lysostaphin for lysis of *S. aureus* cells,[11] and although lysostaphin has proven effective against meticillin-resistant *S. aureus* strains in various animal models,[12] no crystal or NMR structure for any lysostaphin-type protein is available. To our knowledge, even the complete set of Zn-ligands has not been determined.

Here, we present the 1.3 Å crystal structure of full-length LytM, the first structure of a lysostaphin-type metallopeptidase. We report the complete set of Zn^{2+} ligands in LytM, and because this set deviates from prior speculations in the literature, confirm their role by site-directed mutagenesis. Finally, we demonstrate that a truncated form of LytM that roughly corresponds to the mature form of other lysostaphin-related proteases[4,5,13] has much higher specific activity than full-length protein, strongly suggesting that the *lytM* gene encodes a preproenzyme.

Results

LytM expression, purification and crystallisation

Consistent with the extracellular location of the protein, the gene for LytM encodes an export signal at the N terminus. According to SignalP,[14] this leader sequence comprises the first 23 amino acid residues. For heterologous expression in *Escherichia coli*, a cleavage site two residues downstream of the physiological cleavage site is predicted. Here, LytM was expressed with a histidine tag upstream of the natural LytM export sequence. Remarkably, the histidine-tag modified leader sequence was cleaved in *E. coli*, resulting in a protein with the N-terminal sequence AETTN… as shown by ESI mass spectrometry and protein fingerprinting, consistent with the SignalP prediction. The protein was purified and crystallised as described in Materials and Methods. The structure was then solved by multiple wavelength anomalous diffraction (MAD) on a single selenomethionine-containing crystal exploiting the anomalous signal from both the zinc and the selenium atoms.

LytM fold

The crystal structure shows that LytM is a two-domain protein. The N-terminal domain (shown at the bottom of Figure 1) is not conserved in lysostaphin-type proteins. Its ordered part in LytM comprises residues 45 to roughly 98 and can be described as a mixed β-sheet that is formed by two β-hairpins connected by an α-helix. The N-domain makes only very limited contacts with the C-domain, and none of its residues is close to the metal centre.

The C-domain (shown at the top of Figure 1) comprises residues 99–316 and can be divided into two ordered regions that are located upstream and downstream of the disordered segment from residue 147 to residue 182. The region upstream of the disordered segment is poorly conserved and mostly coiled with the exception of one helix. It anchors only one of the four Zn^{2+} ligands, N117 (dotted lines in Figure 1). In stark contrast, the region downstream of the disordered segment is well-conserved and rich in secondary structure elements (continuous lines in Figure 1). Its fold is arranged around a central, six-stranded antiparallel β-sheet. In Richardson nomenclature,[15] the topology of this sheet can be described as $+1$, $+4x$, -1, -1, -1. With the exception of N117, all ligands to the Zn^{2+} are anchored on this sheet or in surrounding loops. A second, much smaller antiparallel β-sheet runs essentially parallel with the main β-sheet, but none of its residues contributes to the metal centre (continuous lines in Figure 1).

The zinc-binding site

Although no exogenous Zn^{2+} was added to recombinant LytM, the Zn^{2+} site in the crystals is fully occupied. The identification of the metal ion as Zn^{2+} was confirmed by X-ray fluorescence that showed the expected absorption maximum at the K-edge of Zn^{2+} at 1.283 Å. Contrary to the common
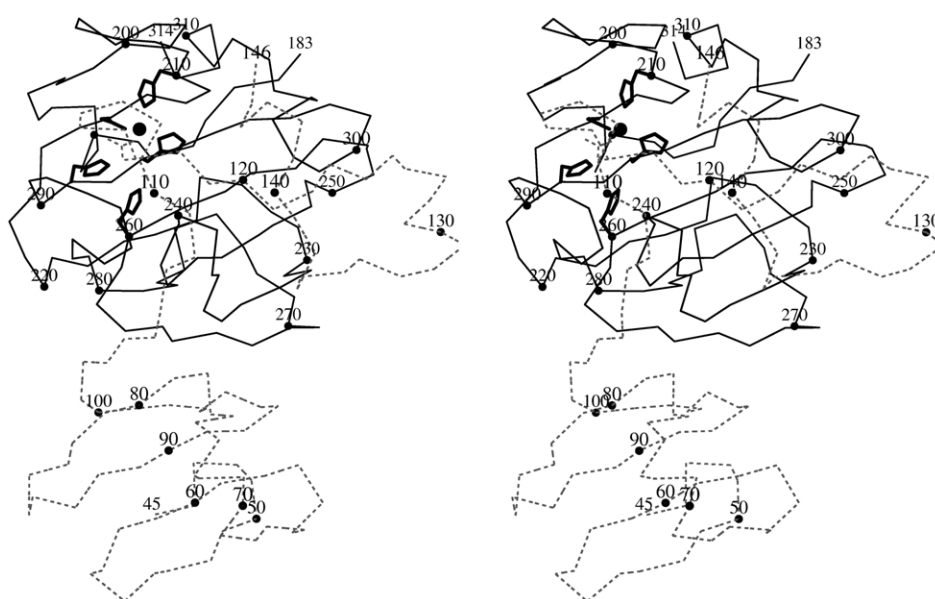
Figure 1. Stereo C$^\alpha$-trace of the LytM structure. The N and C-domains are located at the bottom and top, respectively. Residues of the N-domain and of the C-domain upstream of the disordered segment are represented by dotted lines (45–146). The C$^\alpha$-trace for residues downstream of the disordered segment (183–314) is presented as drawn lines and corresponds roughly to the active protease. Side-chains for some important active-site residues are also presented.

assumption that both histidine residues of the HxH signature sequence are ligands for the Zn^{2+},[2] all atoms in the imidazole ring of the first histidine of the HxH motif are at least 4 Å away from the Zn^{2+} and thus clearly not directly involved in Zn^{2+} chelation.

As shown in Figure 2, the Zn^{2+} in our crystals is tetrahedrally coordinated by N117, H210, D214 and H293, the second histidine residue of the HxH motif. Both histidine residues that act as ligands for the Zn^{2+} donate a hydrogen bond from the imidazole nitrogen that does not contact the metal. This common, so-called elec-His-Zn motif orients the imidazole ring in space and is believed to make it more basic and thus a better ligand to the metal.[16] In H210, the imidazole N$^\varepsilon$ coordinates the Zn^{2+}, and the N$^\delta$ donates a hydrogen bond to the carbonyl oxygen of P200. In H293, it is the N$^\delta$

that coordinates the Zn^{2+}, and the N$^\varepsilon$ that donates a hydrogen bond to the oxygen of the terminal carboxamide of Q295 (see Figure 2). As elec-His-Zn motifs are thought to be favourable, Q295 should be conserved. This is indeed the case, but with a remarkable twist: in a substantial number of lysostaphin-type proteins, Q295 is replaced with glutamic acid that we presume to be in the same conformation and to act as a hydrogen bond acceptor. As residue Q295 is located just two residues downstream of the HxH motif, the signature sequence is better described as HxHxQ/E.

LytM latency

The most unusual feature of the LytM crystal structure is the lack of an ordered water molecule in the coordination sphere of the Zn^{2+}. At 1.3 Å
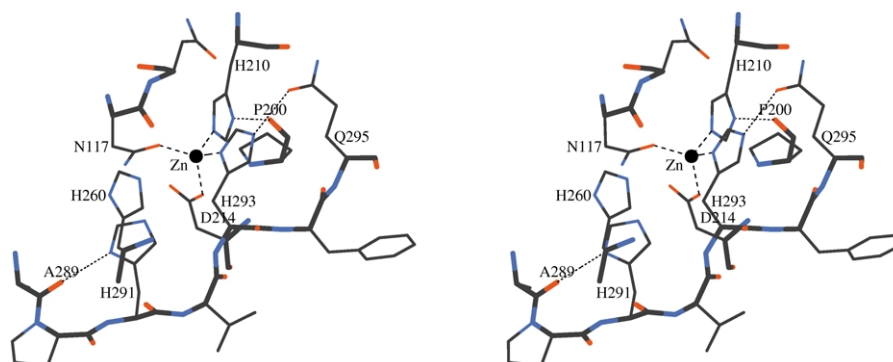
Figure 2. Stereo view of the Zn^{2+}-binding site in LytM. The main-chain trace is drawn with bold lines, side-chains are presented with thin lines. The signature sequence HxHxE/Q runs from left to right in the foreground, and contains H291, H293 and Q295. Interactions between the Zn^{2+} and its ligands are shown with broken lines, and hydrogen bonds that are donated from histidine residues 210, 291 and 293 are presented as dotted lines.

resolution, the absence of electron density for an ordered water molecule that could ligand the Zn^{2+} is significant, all the more so since the tetrahedral geometry of Zn^{2+} coordination by four amino acid ligands leaves no space for a water molecule or substrate carbonyl oxygen to contact the Zn^{2+} directly. Thus, the metal centre cannot be catalytic in the form found in the crystal structure.

As the evidence in the literature for a metal-dependent mechanism of lysostaphin-type proteins activity is firm[10,17] and because we could not find any alternative proteolytic dyad or triad, we focused on the possibility of structural rearrangements of the active-site for peptidase activation. Several lines of evidence suggested that the asparagine residue N117 was most likely to be involved in the changes. Firstly, systematic database searches show that histidine is the most common ligand for Zn^{2+}, followed by glutamic acid, aspartic acid and cysteine.[18] In contrast, asparagine is an unusual ligand for a catalytic Zn^{2+} site. Secondly, the two Zn^{2+} chelating histidine residues in LytM are strongly conserved, the aspartic acid is moderately conserved, and the asparagine is not conserved at all (alignment not shown). Thirdly, the asparagine is the only Zn^{2+} ligand that is located upstream of a large, 40 residue segment in the crystal structure that is disordered, suggesting that N117 itself could be easily moved without disrupting structural integrity of the protein. Finally and most importantly, a profragment roughly comprising the residues upstream and inside the disordered sequence in our crystal structure is known to be cleaved off in other lysostaphin-type peptidases (alignments not shown).[4,19]

Further supporting this idea, we noted that degradation fragments in our LytM preparations appeared to be active (data not shown). Catalytically active degradation products in LytM preparations from both native and recombinant sources have been noted before.[9] Based on their migration behaviour in zymography, Ramadurai et al. assigned molecular masses of 19 kDa and 22 kDa.[9] Consistent with their report, we also find degradation products in our recombinant preparations from E. coli. However, mass spectrometry yields molecular masses of 14.8 kDa for the dominant fragment, substantially less than assigned by Ramadurai et al.[9] and implying a cleavage site downstream of the asparagine Zn^{2+} ligand.

Experimental LytM activation

We therefore hypothesized that a C-terminal fragment of LytM that lacks the asparagine ligand to the Zn^{2+} should be more active than the wild-type. For the definition of the C-terminal fragment, we took guidance from the crystal structure and expressed the fragment of LytM downstream of the disordered region in our crystals with an N-terminal histidine tag. The resulting protein comprises residues 185–316 of the wild-type sequence that together have a molecular mass of 14.4 kDa. A slightly longer, 14.7 kDa fragment could be generated by trypsin-mediated cleavage of full-length LytM. Cleavage occurs between K179 and A180, consistent with the preference of trypsin for basic residues in P1 position of the substrate. As a control, the complete C-domain (LytM 99-316) that contains all four amino acid ligands to the Zn^{2+} was also tested (for an overview of the constructs, see Figure 3).

The results of a thin layer chromatography (TLC)-based pentaglycine degradation assay with equimolar amounts of the different proteins are presented in Figure 4A. Under assay conditions, full-length LytM has no detectable activity (see lane LytM full-length). The same is true of the truncated protein that lacks the entire N-domain, but still contains the full C-domain including the asparagine ligand N117 (see lane LytM 99-316). In marked contrast, the protein that begins just downstream of the disordered region in LytM and lacks N117 shows clear activity and seems to split pentaglycine into di- and triglycine (see lane LytM 185-316). The same result is obtained when LytM is processed with trypsin (see lane LytM + trypsin). A control reaction confirms that trypsin itself is inactive against the pentaglycine substrate, as expected from its specificity (not shown).

Gratifyingly, the active truncation mutant LytM 185-316 shows the inhibitor sensitivity that would be expected for a metallopeptidase (see Figure 4B). 10 mM EDTA, 1 mM 1,10-phenanthroline, glycine hydroxamate the divalent metal ions Zn^{2+} and Hg^{2+} inhibit the activity. In contrast, the epoxide-based cysteine protease inhibitor E64 has no effect, and PMSF inhibits only partially. It has been stated in the literature that $(NH_4)_2SO_4$ and glucosamine inhibit the activity of LytM.[10] Consistent with this report, 10 mM of either $(NH_4)_2SO_4$
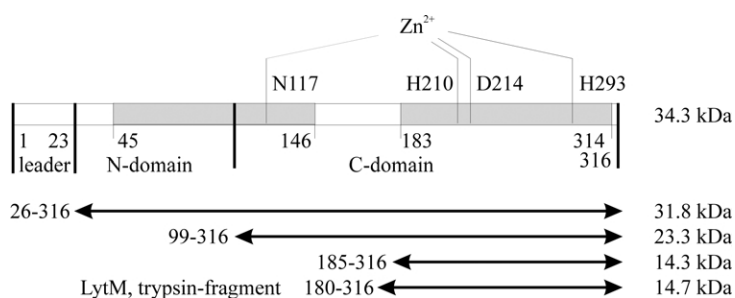
Figure 3. Overview of the domain organisation of LytM and of the truncation constructs that were generated for activity tests. Domain boundaries are indicated with long vertical bars. Grey boxes indicate ordered regions in the crystal structure. On the right, the molecular masses of the different constructs are listed.
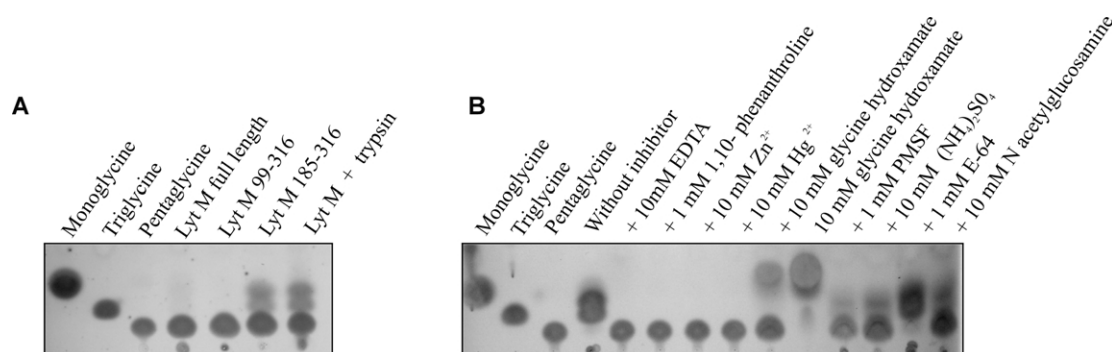
Figure 4. Thin-layer chromatography pentaglycine digestion assay. A, Comparison of the activities of full-length LytM, the C-domain of LytM 99-316, the region downstream of the disordered segment of LytM 185-316 and of trypsin-cleaved LytM. B, Inhibitor sensitivity of truncated LytM 185-316. Unlike all other inhibitors, glycine hydroxamate stains with ninhydrin. Therefore, a control lane "glycine hydroxamate" (without the + sign) with glycine hydroxamate only has been included in the panel. The lane + glycine hydroxamate (with the + sign) shows the result of mixing the inhibitor with enzyme and substrate, just as for all other inhibitors.

or *N*-acetylglucosamine, the variant of glucosamine that is part of the muramic acid peptidoglycan backbone, cause substantial LytM inhibition, although a clear residual activity remains in our hands.

Mutagenesis of the Zn^{2+} chelating asparagine

To our knowledge, an asparagine-mediated latency mechanism is novel in metalloproteases. To test our prediction that the asparagine has an inhibitory role, we replaced the asparagine Zn^{2+} ligand with alanine. Consistent with our expectations, we find that the full-length mutant has activity in three different functional assays. The activity is robust in the TLC pentaglycine degradation assay (see Figure 5A), and clearly above background in zymography and the Remazol dye assays (see Figure 5B and C). We assume that the higher substrate concentration in the TLC assay helps to displace the mutant inhibitory region of the enzyme. For the zymography and Remazol dye assays, the substrate concentration is much lower, and the active-site is probably still partially occluded by the N-terminal part of the enzyme, even though the specific interaction with the Zn^{2+} has been disrupted. Trypsin cleavage enhances the activity of the N117A mutant to the level observed with cleaved wild-type enzyme (see Figure 5C, note that all activities are relative to cleaved wild-type enzyme). This is expected, because the C-terminal cleavage products from wild-type enzyme and mutant enzyme are identical.

Mutagenesis of Zn^{2+} chelating residues in active LytM

The three Zn^{2+} ligands that we expect to be present in active enzyme, H210, D214 and H293, are conserved in lysostaphin-type sequences, but all three occur outside the YxHx(11)Vx(12/20)Gx(5-6)H[10,20] signature motif for lysostaphin-type peptidases, and two of them, H210 and D214,

have not been considered as Zn^{2+} ligands before to the best of our knowledge. Instead, it was speculated that the two histidine residues of the HxH signature motif would contact the Zn^{2+} directly,[2] both because of an analogy with carboanhydrase[4] and because the first histidine of the HxH motif was shown to be essential for activity.[19]

To test the relevance of the LytM structure for the situation in solution, we mutated the three Zn^{2+} ligands individually to alanine in the context of full-length LytM. All three constructs could be expressed, and two of them, H210A and D214A yielded soluble proteins. Consistent with our expectations, the mutant proteins were inactive both before and after the trypsin cleavage step in the pentaglycine (see Figure 5A, left panel), zymography (see Figure 5B, left panel) and Remazol dye (see Figure 5C) assays. The third mutant, H293A was expressed in good yield, but was entirely insoluble. An attempt to express the H293A mutation in the context of truncated LytM 185-316 again gave insoluble protein, clearly showing the importance of H293 for folding and supporting a role for this residue in Zn^{2+} chelation.

Mutagenesis of the first histidine of the HxH motif

The first histidine of the HxH motif, H291, is clearly not a ligand for the Zn^{2+} in the LytM crystal structure. Nevertheless, its strong conservation among lysostaphin-type peptidases clearly suggests a functional role for this residue. To test this hypothesis, we replaced this histidine with alanine. Consistent with our expectation, the resultant LytM mutant is devoid of activity in the pentaglycine assay (see Figure 5A, right panel) and in zymography (see Figure 5B, right panel), both before and after truncation with trypsin. Consistent with these results, at best residual activity is observed in the Remazol dye assay (see Figure 5C).
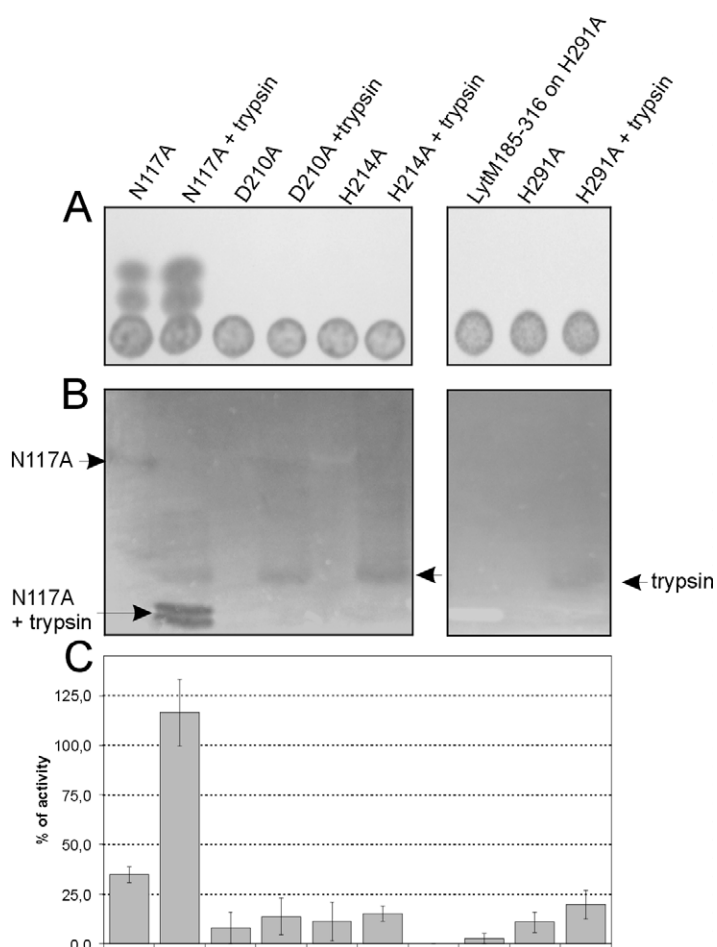
Figure 5. Activity of LytM mutants in three different assays. A, Pentaglycine degradation assay. B, Zymography with purified *S. aureus* peptidoglycans. Note that bands of activity appear as black stripes, because gels were not stained and instead photographed against a black background with illumination from the back. C, Remazol dye release assay. All activities are relative to the activity of trypsin-cleaved LytM. Standard deviations are derived from eight independent measurements.

Discussion

LytM and glucose permease domain IIA have similar folds

Automated, quantitative DALI[21] structure comparisons between LytM and all proteins in the Protein Data Bank (PDB) identified a highly significant (DALI Z-score 7.2) similarity of almost the entire C-domain of LytM to 1GPR, the structure of glucose permease domain IIA from *Bacillus subtilis*[22] (see Figure 6). The glucose permease domain IIA is part of a phosphorylation dependent carbohydrate transport system, and is believed to act as a phosphorous shuttle that can transiently accept a phosphate on one of its histidine residues.[22] Superposition of 1GRP with LytM shows that the active-site of the glucose permease is substantially away from the LytM metal centre (see Figure 6), and that the active histidine in 1GPR is not conserved in LytM. Conversely, glucose permease domain II is not known to bind Zn^{2+}, and lacks the Zn^{2+} ligands that are present in the LytM structure. Taken together, it appears that the catalytic activities have evolved independently even if there was a common ancestor that would explain the similarity in fold.

We also noted a similarity between LytM and PDB-entry 1LBU (P. Wery, PhD thesis) that contains a revised version of the structure of the D-Ala-D-Ala carboxypeptidase from *Streptomyces albus G*.[23] This similarity went undetected in global DALI-based fold comparisons because it is restricted to a core folding motif around the active-site and to the conservation of active-site residues. Its details and implications will be discussed elsewhere.

LytM *versus* HExxH metalloproteases

It is interesting to compare LytM, and by implication, lysostaphin-like metallopeptidases, with zincins, the prototypical and most studied HExxH metalloproteases. In zincins, the two histidine residues in the signature motif serve invariably as Zn^{2+} ligands, that together with either a histidine (e.g. metzincins) or a glutamate (gluzincins) and the nucleophilic water molecule form the trigonal-pyramidal coordination sphere of the catalytic Zn^{2+} centre.[1,24] In some cases, a fourth amino acid ligand extends the coordination sphere to trigonal-bipyramidal geometry.[25] Mechanistically, the Zn^{2+} in HExxH metalloproteases is believed to polarise the carbonyl group of the scissile amide bond, and the conserved glutamate residue together with the metal ion is thought to polarise a water molecule for nucleophilic attack.[24]

In contrast with zincins, only the second histidine of the HxH-motif is in contact with the Zn^{2+}

in LytM. The strong, although not universal conservation of the first histidine of this motif clearly suggests a catalytic role for this residue. In support of this hypothesis, we have shown that replacement of the first histidine of the HxH motif with alanine abolishes LytM activity in three different assays. The LytM result is consistent with a previous mutagenesis study on LasA, another lysostaphin-type peptidase, which concluded that H120 of LasA, the equivalent of H291 of LytM and the first histidine of the HxH motif, is essential for activity.[19] Several interpretations of this result are possible: as LytM contains no glutamate residue in the active-site, it is tempting to speculate that the first conserved histidine of the HxH motif is the functional equivalent of the glutamate in HExxH metalloproteases and thus has a role in the activation of the incoming water molecule. However, we caution that another conserved histidine in lysostaphin-type peptidases, H260 in LytM, is equally close to the metal centre and could also play this role. In the absence of a crystal structure of active LytM in complex with a substrate analogue, other less likely roles for one or both of these histidine residues remain possible, for example in the stabilisation of a reaction intermediate.

An asparagine switch?

Like LytM, matrix metalloproteases (MMPs) are secreted in a latent form. MMP activation occurs by a variety of disparate means, including protease treatment, conformational perturbants such as sodium dodecyl sulphate, heavy metals such as Hg^{2+} and sulphhydryl-alkylating agents such as *N*-ethylmaleimide.[26] All these activation mechanisms were traced back to the displacement of a cysteine residue of the profragment from the catalytic Zn^{2+} centre, an activation mechanism that van Wart and Birkedal-Hansen termed the "cysteine switch".[26] The cysteine switch mechanism has been confirmed by structural studies. In the proforms of both latent gelatinase A (pro-MMP-2)[27] and latent stromelysin-I (pro-MMP-3),[28] the sulphur of a cysteine of the profragment is directly liganded to the catalytic Zn^{2+}. In the mature forms, the place of the cysteine sulphurs is taken by a solvent molecule or by a Zn^{2+} chelating group of an inhibitor.[28,29] Because of the analogy with the cysteine switch in MMPs, we suggest the term "asparagine switch" for the latency mechanism of LytM. The poor conservation of the asparagine in lysostaphin-like enzymes makes it likely that residues other than asparagine can act as the switch in other family members, so that the broader latency mechanism of lysostaphin-type peptidases will eventually turn out to be a "Zn^{2+} ligand switch".

Is full-length LytM active?

The prior literature on LytM consistently assumes that the full-length enzyme is the active species.[9,10] Experimentally, Ramadurai *et al.* have shown that their LytM preparations give rise to three bands in zymography, one corresponding to the full length enzyme and two bands at 19 kDa and 22 kDa that they identify as degradation products.[9] To our knowledge, these authors never
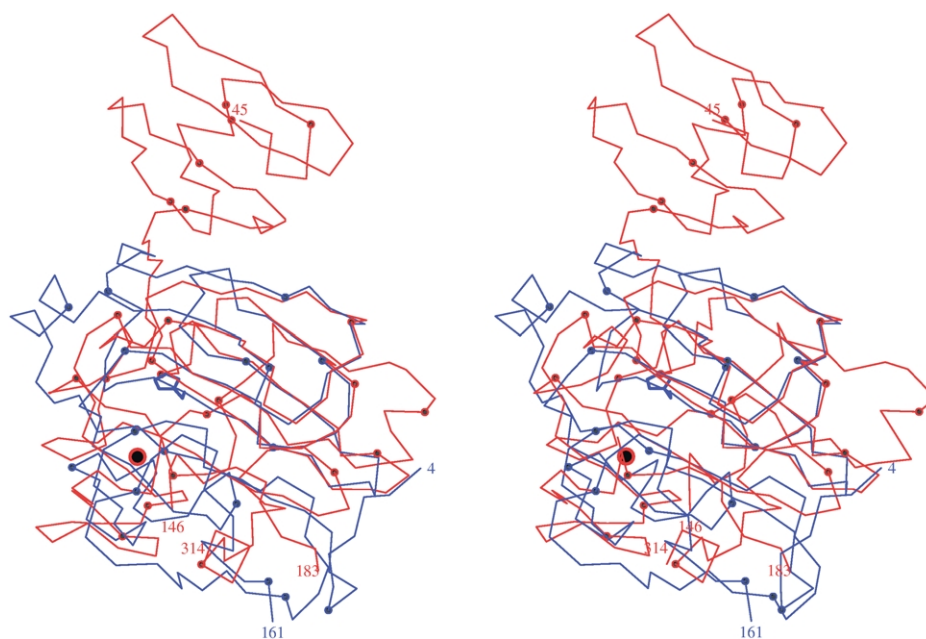
Figure 6. Superposition of the C$^\alpha$ traces of LytM (red lines) and glucose permease domain IIA (blue lines). The correspondence between the two proteins extends essentially over the entire C-terminal domain of LytM. In both structures, every tenth residue is marked with a dot. The Zn^{2+} in LytM is shown as a red sphere with black centre, and the histidine in glucose permease domain IIA that can be phosphorylated is drawn in ball-and-stick representation.

quantified the specific activity of the different peptidase forms. In our hands, the full-length protein has residual activity at best, and only the truncated enzyme yields a robust zymography signal (data not shown). The published zymography results with equally intense bands for all three forms of protease could thus be due to a large amount of LytM and a small amount of degraded enzyme. Alternatively, it is possible that activation occurred during the renaturation step after denaturing gel electrophoresis, although this does not happen to an appreciable extent in our hands. We also noted that the specific activity of full-length LytM preparations grows over time, especially in samples that were contaminated with other proteins from *E. coli*. Gratifyingly, this increase in activity correlates with increasing amounts of degraded LytM in these preparations.

Is LytM processed *in vivo*?

The much higher specific activity of truncated LytM suggests that the enzyme could be processed *in vivo*, an assumption that would be consistent with the known processing to activate other lysostaphin-type proteins.[4,5,13] Nevertheless, the conclusion is not inevitable. LytM is thought to be an autolysin with a role in actively growing and dividing cells.[10] As the enzyme acts on the producer organism, a tight control of its activity should therefore be desirable, and transient activation could happen through mechanisms other than proteolysis. It would be conceivable that full-length LytM is an enzyme with a "lid" that is displaced by certain substrates only, although the near-complete lack of activity of the enzyme in our assays does not support this conclusion. The disordered LytM region in the crystal structure and the processing of LytM by the non-physiological activator trypsin and by protease contaminations from the heterologous host *E. coli* all suggest that many proteases from *S. aureus* would probably also activate LytM *in vitro*. Thus, to fully confirm the profragment hypothesis, the exact cleavage that occurs *in vivo* will have to be reproduced *in vitro*. Alternatively, the profragment hypothesis could be proven by a knockout that abolishes LytM processing *in vivo*. Work in this direction is under way.

Materials and Methods

Cloning, protein expression and purification

LytM sequences from various strains of *S. aureus* have been deposited in sequence databases, and two alternative start codons have been assigned.[9,30] We favour the second ATG as the start codon because of the presence of a Shine-Dalgarno sequence ten nucleotides upstream and assume for counting purposes that the translation product has the sequence MKKL… and refer to the methionine upstream of the two lysine residues as residue 1. Standard PCR techniques were used to amplify the *lytM* gene from genomic DNA of *S. aureus* strain NCTC8325. The gene was cloned into a derivative of pET15b, named pET15bmod, that lacks the original *Eco*RI site and contains a newly introduced *Eco*RI site in place of the original thrombin cleavage site. For protein expression, BL21 (DE3) cells carrying the plasmid were grown to an A_{600} of 0.7, induced with 1 mM IPTG and shifted to 28 °C for up to six hours. For expression of the selenomethionine variant of the protein, the plasmid was transformed into BL834 (DE3), the methionine auxotrophic parent strain of BL21 (DE3). A small scale overnight culture was grown in NMM medium containing 0.3 mM L-methionine, and used to inoculate the full scale culture in NMM containing 0.3 mM D,L-selenomethionine. Cells were grown to an A_{600} of 1.5, and kept at 28 °C for six hours after induction with 1 mM IPTG.[31]

Cells were harvested and resuspended in buffer A (20 mM Tris (pH 7.5), 50 mM NaCl). After sonification and clarificaiton of the lysate, the supernatant was applied to a DEAE Sepharose FF column (Amersham Pharmacia, 30 ml column volume) equilibrated in buffer A. The protein was recovered 90% pure in the flow through. After concentration (Amicon 10 kDa cut-off regenerated cellulose filters), the protein was subjected to a gel filtration step on Sephacryl S-300 HR (Amersham Pharmacia) in 5 mM Tris (pH 7.5). LytM migrated as a monomer. The selenomethionine variant behaved indistinguishably from the wild-type. Therefore, mass spectrometry was used to confirm the incorporation of selenomethionine prior to synchrotron data collection.

Crystallisation

Crystals were grown in sitting drops at 21 °C by equilibrating a 1:1 mixture of protein (around 40 mg/ml in 5 mM Tris, pH 7.5) and reservoir buffer against reservoir buffer containing 170 mM ammonium sulphate, 25.5% (w/v) PEG 8K and 15% (v/v) glycerol. Crystals appeared after three or four days, belonged to space group *P*12(1)1 with cell constants

Table 1. Data collection and refinement statistics

Data collection statistics		Refinement statistics	
Space group	*P*12(1)1	*R*-factor (%)	16.4
a (Å)	45.33	*R*-free (%)	18.1
b (Å)	53.23	rmsd bond distance (Å)	0.01
c (Å)	51.60	rmsd angles (deg.)	1.3
β	104.02	*B* (isotropic) from Wilson	12.7
Independent reflections	54 733		
Resolution (Å)	1.3	Ramachandran core (%)	92.3
Completeness (%)	94	Ramachandran additionally all (%)	7.7
R_{sym} (%) (last shell in brackets)	6.2 (17.4)	Ramachandran generously all (%)	0.0
I/σ (last shell in brackets)	6.4 (3.5)	Ramachandran disallowed (%)	0.0

45.33 Å × 53.23 Å × 51.60 Å, 90° × 104.02° × 90° and contained one molecule of LytM per asymmetric unit. They could be flash-frozen directly from mother liquor and diffracted in-house to about 1.7 Å and to 1.3 Å on BL2, BESSY, Berlin. For the deposited dataset, the high-resolution pass was collected on BESSY and the low-resolution pass in-house on a separate specimen. The crystallographic quality factors for the combined dataset are excellent and are summarised in Table 1.

Structure determination

The structure was determined by two-wavelength MAD on a single selenomethionine crystal, collecting data at the absorption maximum of Se ($\lambda = 0.979857$ Å, $f'_{exp} = -7.8$, $f'_{exp} = 4.3$) and Zn ($\lambda = 1.282713$ Å, $f'_{exp} = -7.2$, $f'_{exp} = 4.0$) to 1.9 Å resolution. Anomalous difference Patterson maps showed very clear contrast for both absorption maxima, with one Zn-site standing out in the $\lambda = 1.282713$ Å anomalous map. Cross-phasing the anomalous data at the selenium absorption edge with phases derived from the Zn-site identified selenium positions in the anomalous difference Fourier map with very clear signal, but sites on both hands were still present. Selenium–selenium cross-vectors in the $\lambda = 0.979857$ Å anomalous difference Patterson map were used to split the set of candidate selenium positions into two sets with consistent hand, giving four possible heavy atom arrangements for the phasing procedure: two choices for the hand of the Zn site, and then two choices each for the hand of the selenium sites. One choice led to a very clear map that could be interpreted automatically by the ARP/WARP procedure, while all three other choices gave uninterpretable maps. The final model comprises 234 residues, namely residues 45–146 and residues 183–314 (the initiator methionine is taken as residue 1). This implies that 19 residues that are chemically present at the N terminus of our molecule are disordered. The same applies for the 36 residues 147–182 and for the two most C-terminal residues. In spite of the rather large number of disordered residues, R_{cryst} and R_{free} at 1.3 Å resolution are satisfactory (see Table 1). The model has reasonable stereochemistry and the sites of methionine sulphur atoms are consistent with the selenium positions used for phasing, once more confirming the sequence assignment.

Mutagenesis

LytM mutants N117A, H210A, D214A and H293A were generated by PCR-based site-directed mutagenesis according to the Stratagene protocol with *Pfu Turbo* DNA polymerase (Stratagene). Truncated versions of LytM were generated by cloning corresponding PCR fragments into the expression vector pET15mod. The resulting constructs LytM 99-316 and LytM 185-316 started at A99 and H185, respectively. As the H293A mutation in the context of full-length LytM yielded insoluble protein, this mutation was also introduced in the context of the LytM 185-316 construct, but unfortunately again yielded only insoluble protein. Full-length soluble point mutants were purified as the wild-type protein. Truncated versions were expressed with an N-terminal histidine tag, applied in buffer A to Ni–NTA agarose (Quiagen), washed with 50 mM imidazole in buffer A and eluted with 300 mM imidazole, again in buffer A and subsequently subjected to a gel filtration step on Sephacryl S-300 HR (Amersham Pharmacia).

Trypsin digest

Proteins (20 μg) were digested with 0.1 unit of trypsin (Sigma) for ten minutes at 37 °C. The reaction was stopped by adding benzamidine to the final concentration of 5 mM.

Peptidoglycan isolation

Peptidoglycans were isolated from *S. aureus* ATCC25923. Autoclaved cells were washed twice in buffer A and then incubated in 4% SDS, first at room temperature for 90 minutes and then at 100 °C for 20 minutes. Insoluble material was extensively washed with buffer A and finally resuspended in 10% trichloro-acetic acid (TCA) and incubated at 4 °C for 48 hours with gentle shaking. Harvested insoluble material was then treated with 2 mg/ml of Pronase (Sigma) in buffer A for one hour at 60 °C. After extensive washing in the same buffer, peptidoglycans were resuspended in buffer A and used for further experiments or stored at −20 °C.

Zymography

The enzyme was assayed for activity on a 12% (w/v) polyacrylamide-sodium dodecyl sulphate gel containing 0.2% (w/v) peptidoglycans isolated from *S. aureus* as described above. About 3 μg of the analysed protein was loaded on each lane. The gels were incubated for two to four hours at 37 °C in 20 mM Tris–HCl (pH 7.5), containing 2.5% Triton X-100 to permit protein renaturation. Lytic zones appeared as clear bands within the opaque gel. For photos, the gel was held on a glass plate against a sheet of black paper, with illumination from the back.

TLC

Pentaglycine (5 mM, Sigma) was incubated for five hours at 37 °C with enzyme samples (1 μg/μl) in a total volume of 20 μl in 10 mM Tris–HCl buffer (pH 7.5). Subsequently, 5 μl samples of the reaction were applied on a TLC plate covered with Silica Gel 60 (Merck) and developed with a mixture of *n*-butanol:acetic acid:water (4:1:1, by vol.). To visualise the spots, the plate was sprayed with 0.2% ninhydrin in ethanol and heated to 100 °C.

Remazol dye release assay

The Remazol dye release assay was done as described by Zhou *et al.*[32] Briefly, Remazol Brilliant Blue (RBB, Sigma) derivatives were prepared by suspending insoluble peptidoglycans in 250 mM NaOH containing 20 mM RBB and incubating them first at 37 °C for six hours and then at 4 °C for 12 hours. Dyed products were washed extensively until a colourless supernatant was obtained. The dye release assays were done for 12 hours at 37 °C in buffer A, at a substrate concentration of 3 mg/ml and at an enzyme concentration of 0.05 μg/ml. Reactions were stopped by adding half the volume of 96% ethanol, insoluble material was removed by centrifugation and the absorbance was measured at 595 nm.

Atomic coordinates

Structure factors and coordinates have been deposited

in the PDB and will be available on publication under accession code 1QWY.

References

1. Hooper, N. M. (1994). Families of zinc metalloproteases. *FEBS Letters*, **354**, 1–6.
2. Rawlings, N. D., O'Brien, E. & Barrett, A. J. (2002). MEROPS: the protease database. *Nucl. Acids Res.* **30**, 343–346.
3. Barrett, A. J., Rawlings, N. D. & Woessner, J. F. (1998). *Handbook of Proteolytic Enzymes*, Academic Press, London.
4. Li, S. L., Norioka, S. & Sakiyama, F. (1990). Molecular cloning and nucleotide sequence of the beta-lytic protease gene from *Achromobacter lyticus*. *J. Bacteriol.* **172**, 6506–6511.
5. Peters, J. E. & Galloway, D. R. (1990). Purification and characterization of an active fragment of the LasA protein from *Pseudomonas aeruginosa*: enhancement of elastase activity. *J. Bacteriol.* **172**, 2236–2240.
6. DeHart, H. P., Heath, H. E., Heath, L. S., LeBlanc, P. A. & Sloan, G. L. (1995). The lysostaphin endopeptidase resistance gene (epr) specifies modification of peptidoglycan cross bridges in *Staphylococcus simulans* and *Staphylococcus aureus*. *Appl. Environ. Microbiol.* **61**, 1475–1479.
7. Beukes, M. & Hastings, J. W. (2001). Self-protection against cell wall hydrolysis in *Streptococcus milleri* NMSCC 061 and analysis of the millericin B operon. *Appl. Environ. Microbiol.* **67**, 3888–3896.
8. Smith, T. J., Blackman, S. A. & Foster, S. J. (2000). Autolysins of *Bacillus subtilis*: multiple enzymes with multiple functions. *Microbiology*, **146**, 249–262.
9. Ramadurai, L. & Jayaswal, R. K. (1997). Molecular cloning, sequencing, and expression of lytM, a unique autolytic gene of *Staphylococcus aureus*. *J. Bacteriol.* **179**, 3625–3631.
10. Ramadurai, L., Lockwood, K. J., Nadakavukaren, M. J. & Jayaswal, R. K. (1999). Characterization of a chromosomally encoded glycylglycine endopeptidase of *Staphylococcus aureus*. *Microbiology*, **145**, 801–808.
11. Zygmunt, W. A., Browder, H. P. & Tavormina, P. A. (1967). Lytic action of lysostaphin on susceptible and resistant strains of *Staphylococcus aureus*. *Can. J. Microbiol.* **13**, 845–853.
12. Climo, M. W., Patron, R. L., Goldstein, B. P. & Archer, G. L. (1998). Lysostaphin treatment of experimental methicillin-resistant *Staphylococcus aureus* aortic valve endocarditis. *Antimicrob. Agents Chemother.* **42**, 1355–1360.
13. Thumm, G. & Gotz, F. (1997). Studies on prolysostaphin processing and characterization of the lysostaphin immunity factor (Lif) of *Staphylococcus simulans* biovar staphylolyticus. *Mol. Microbiol.* **23**, 1251–1265.
14. Nielsen, H., Engelbrecht, J., Brunak, S. & von Heijne, G. (1997). Identification of prokaryotic and eukaryotic signal peptides and prediction of their cleavage sites. *Protein Eng.* **10**, 1–6.
15. Richardson, J. S. (1977). beta-Sheet topology and the relatedness of proteins. *Nature*, **268**, 495–500.
16. Alberts, I. L., Nadassy, K. & Wodak, S. J. (1998). Analysis of zinc binding sites in protein crystal structures. *Protein Sci.* **7**, 1700–1716.
17. Kessler, E., Safrin, M., Abrams, W. R., Rosenbloom, J. & Ohman, D. E. (1997). Inhibitors and specificity of *Pseudomonas aeruginosa* LasA. *J. Biol. Chem.* **272**, 9884–9889.
18. Vallee, B. L. & Auld, D. S. (1990). Zinc coordination, function and structure of zinc enzymes and other proteins. *Biochemistry*, **29**, 5647–5659.
19. Gustin, J. K., Kessler, E. & Ohman, D. E. (1996). A substitution at His-120 in the LasA protease of *Pseudomonas aeruginosa* blocks enzymatic activity without affecting propeptide processing or extracellular secretion. *J. Bacteriol.* **178**, 6608–6617.
20. Sugai, M., Fujiwara, T., Akiyama, T., Ohara, M., Komatsuzawa, H., Inoue, S. & Suginaka, H. (1997). Purification and molecular characterization of glycylglycine endopeptidase produced by *Staphylococcus capitis* EPK1. *J. Bacteriol.* **179**, 1193–1202.
21. Holm, L. & Sander, C. (1995). Dali: a network tool for protein structure comparison. *Trends Biochem. Sci.* **20**, 478–480.
22. Liao, D. I., Kapadia, G., Reddy, P., Saier, M. H., Jr, Reizer, J. & Herzberg, O. (1991). Structure of the IIA domain of the glucose permease of *Bacillus subtilis* at 2.2 Å resolution. *Biochemistry*, **30**, 9583–9594.
23. Dideberg, O., Charlier, P., Dive, G., Joris, B., Frere, J. M. & Ghuysen, J. M. (1982). Structure of a Zn2 + -containing D-alanyl-D-alanine-cleaving carboxypeptidase at 2.5 Å resolution. *Nature*, **299**, 469–470.
24. Bode, W., Gomis-Ruth, F. X. & Stockler, W. (1993). Astacins, serralysins, snake venom and matrix metalloproteinases exhibit identical zinc-binding environments (HEXXHXXGXXH and Met-turn) and topologies and should be grouped into a common family, the "metzincins". *FEBS Letters*, **331**, 134–140.
25. Stocker, W. & Bode, W. (1995). Structural features of a superfamily of zinc-endopeptidases: the metzincins. *Curr. Opin. Struct. Biol.* **5**, 383–390.
26. Van Wart, H. E. & Birkedal-Hansen, H. (1990). The cysteine switch: a principle of regulation of metalloproteinase activity with potential applicability to the entire matrix metalloproteinase gene family. *Proc. Natl Acad. Sci. USA*, **87**, 5578–5582.
27. Morgunova, E., Tuuttila, A., Bergmann, U., Isupov, M., Lindqvist, Y., Schneider, G. & Tryggvason, K. (1999). Structure of human pro-matrix metalloproteinase-2: activation mechanism revealed. *Science*, **284**, 1667–1670.
28. Becker, J. W., Marcy, A. I., Rokosz, L. L., Axel, M. G., Burbaum, J. J., Fitzgerald, P. M. *et al.* (1995).

Stromelysin-1: three-dimensional structure of the inhibited catalytic domain and of the C-truncated proenzyme. *Protein Sci.* **4**, 1966–1976.

29. Feng, Y., Likos, J. J., Zhu, L., Woodward, H., Munie, G., McDonald, J. J. *et al.* (2002). Solution structure and backbone dynamics of the catalytic domain of matrix metalloproteinase-2 complexed with a hydroxamic acid inhibitor. *Biochim. Biophys. Acta*, **1598**, 10–23.

30. Baba, T., Takeuchi, F., Kuroda, M., Yuzawa, H., Aoki, K., Oguchi, A. *et al.* (2002). Genome and virulence determinants of high virulence community-acquired MRSA. *Lancet*, **359**, 1819–1827.

31. Budisa, N., Steipe, B., Demange, P., Eckerskorn, C., Kellermann, J. & Huber, R. (1995). High-level biosynthetic substitution of methionine in proteins by its analogs 2-aminohexanoic acid, selenomethionine, telluromethionine and ethionine in *Escherichia coli*. *Eur. J. Biochem.* **230**, 788–796.

32. Zhou, R., Chen, S. & Recsei, P. (1988). A dye release assay for determination of lysostaphin activity. *Anal. Biochem.* **171**, 141–144.

Edited by R. Huber